Ralf Zimmermann, Dirk Romeis, Isabelle Bihannic, Martien Cohen Stuart, Jens-Uwe Sommer, Carsten Werner, Jérome F. L. Duval

Electrokinetics as an alternative to neutron reflectivity for evaluation of segment density distribution in PEO brushes

Erstveröffentlichung in / First published in:
Soft Matter. 2014, 10(39), S. 7804–7809 [Zugriff am: 04.11.2019]. Royal Society of Chemistry. ISSN 1744-6848.

DOI: https://doi.org/10.1039/c4sm01315h

Soft Matter

PAPER

View Article Online
View Journal | View Issue

Cite this: *Soft Matter*, 2014, **10**, 7804

Electrokinetics as an alternative to neutron reflectivity for evaluation of segment density distribution in PEO brushes

Ralf Zimmermann,†*[a] Dirk Romeis,[a] Isabelle Bihannic,[b] Martien Cohen Stuart,[c] Jens-Uwe Sommer,[a] Carsten Werner[ad] and Jérôme F. L. Duval†*[b]

Received 18th June 2014
Accepted 11th August 2014

DOI: 10.1039/c4sm01315h

www.rsc.org/softmatter

Unravelling details of charge, structure and molecular interactions of functional polymer coatings defines an important analytical challenge that requires the extension of current methodologies. In this article we demonstrate how streaming current measurements interpreted with combined self consistent field (SCF) and soft surface electrokinetic theories allow the evaluation of the segment distribution within poly(ethylene oxide) (PEO) brushes beyond the resolution limits of neutron reflectivity technique.

1. Introduction

Surface modification with use of end-grafted polymer chains is now a routine procedure adopted for the design of smart materials. It has been the focus of numerous studies in both fundamental and applied research fields.[1,2] In particular, polymer brushes have received a lot of attention due to their facile synthesis and tuneable properties.[3] One of the key issues remains the evaluation and measurement of the polymer segment distribution across polymer brushes in the direction normal to the supporting surface. In their pioneering work, Alexander[4] and de Gennes[5] assumed a homogeneous density of polymer segments throughout the brush (box model). Later, starting from the identification of the most probable polymer conformation, analytical self-consistent field (SCF) theories predicted parabolic brush profiles.[6] Application of numerical SCF theories refined these predictions by revealing larger stretching of the polymer chains due to fluctuations of their conformations, thus resulting in a gradually decreasing polymer density in the outermost region of the brush.[7] With increasing processing power of computers, Monte Carlo[8] and molecular dynamic simulations[9] have been widely used to study the structural details of polymer brushes at a molecular scale under various medium conditions, thus refining the results obtained from SCF formalisms. These various theoretical approaches were confronted to experimental data mainly collected with optical methods, X-ray reflectivity and neutron scattering techniques.[10–13] While results could be satisfactorily collated with theory for a number of systems, it appears that the segment density distribution across brushes cannot be unambiguously derived from neutron reflectivity data analysed according to brush theory.[14] Clearly, alternative techniques are then required to investigate such systems. Building on theoretical and experimental studies by Dukhin, Cohen Stuart and others,[15–20] recent developments in the field of electrokinetics (streaming current/potential) of diffuse soft interfaces allow addressing intertwined electrostatic and structural properties of soft polymer films[21–27] including stimuli-responsive coatings,[21,22] polyelectrolyte layers[23,24] and biohybrid hydrogels.[25] In this study we show that streaming current measurements interpreted on the basis of combined SCF and soft surface electrokinetic theories offer an appropriate alternative for the evaluation of brush profiles, which bypasses the inapplicability of neutron reflectivity for profile evaluation in the range of low to moderate grafting densities. For that purpose, streaming current data collected for PEO brushes[26] with a grafting density of 0.1 nm^{-2} were successfully analysed on the basis of electro-hydrodynamic theory for diffuse soft interfaces[27] with explicit account of the segment density distribution computed according to the SCF method suggested by Milner *et al.*[28] Comparison of theoretical neutron reflectivity patterns obtained with profile parameters issued from the electrokinetic analysis underlines that neutron reflectivity is not suitable for distinguishing between parabolic and polydisperse profiles of brushes of similar or lower grafting density.

[a]*Leibniz Institute of Polymer Research Dresden, Max Bergmann Center of Biomaterials Dresden, Hohe Strasse 6, 01069 Dresden, Germany. E-mail: zimmermn@ipfdd.de*

[b]*CNRS-Université de Lorraine, Laboratoire Interdisciplinaire des Environnements Continentaux (LIEC), UMR 7360, Vandoeuvre-lès-Nancy, F-54501, France. E-mail: jerome.duval@univ-lorraine.fr*

[c]*Laboratory of Physical Chemistry and Colloid Science, Wageningen University, P.O. box 8038, 6700EK Wageningen, The Netherlands*

[d]*Technische Universität Dresden, Center for Regenerative Therapies Dresden, Tatzberg 47, 01307 Dresden, Germany*

† Both authors equally contributed to this work.

2. Experimental section

2.1 Brush preparation

PEO brushes with a grafting density σ of 0.1 nm^{-2} were prepared on top of polystyrene (PS) coated glass substrates applying a Langmuir–Blodgett method reported by Currie

et al.[29] The polymer consists of a PEO block with average 700 monomer units and a PS block of 38 repeat units. The latter was used to anchor the polymer at the polystyrene pre-coated substrate surface.[29] The reported polydispersity (denoted as PD) of the PEO is 1.25.[29]

2.2 Electrokinetic measurements

Streaming current measurements were performed for various salt concentrations and pH values across rectangular streaming channels formed by two sample surfaces (length: $L_o = 20$ mm, width: $\ell = 10$ mm, separation distance $H = 50$ μm) using the Microslit Electrokinetic Set-up.[30,31] The composition of the electrolyte solution was changed by addition of small aliquots of 0.1 M KCl, HCl and KOH solutions. At each condition the electrolyte was equilibrated for about 40 min prior to measurement.

3. Theory and data interpretation

3.1 Calculation of the brush profiles

Normalized brush profiles were calculated for PD = 1 (reference profile for monodisperse brush) and PD = 1.25 (polydisperse brush) on the basis of the SCF method reported in ref. 28 under the assumptions that the chain conformations obey Gaussian statistics and mean field volume interactions are adequately approximated *via* the excluded volume term. In details, the brush profiles were obtained from the numerical solution of the implicit integral eqn (23) given in ref. 28 for moderate density. Since PEO is a very flexible polymer, we performed the SCF calculations in accordance with previous work[32,33] considering symmetric fundamental segments of linear size b. In case of the polydisperse brush, the chain length distribution was approximated by the Schulz–Zimm expression.[34]

For the evaluation of the electrohydrodynamic features of the PEO/electrolyte solution interphase, the normalized segment density profiles were converted into real segment densities using 0.1 nm^{-2} for the grafting density σ, $N_{av} = 700$ for the average number of monomer units per polymer chain and 0.37 nm for the segment length b.[32]

3.2 Electrohydrodynamics of diffuse soft thin-films

The theory for the electrohydrodynamics of diffuse soft thin-films supported by a hard substrate was recently reported by Duval *et al.*[21–27] For practical arrangements of electrokinetic cells, the liquid flow is oriented in the direction parallel to the PEO-grafted surface under action of an applied pressure drop ΔP.[27] The local velocity, $v(x)$, then depends on the dimension perpendicular to the interface, x, according to the generalized Brinkman equation:[35]

$$\frac{d^2V(X)}{dX^2} - \frac{(\lambda_o H)^2 f(X) V(X)}{1 + \frac{3}{4}\phi_o f(X)\left[1 - \left(\frac{8}{\phi_o f(X)} - 3\right)^{1/2}\right]} = -1. \quad (1)$$

Eqn (1) allows an adequate modelling of hydrodynamic flow within polymer materials that are highly to moderately hydrated.[19] In our previous work,[21–24] the analysis was carried out using only the first term in the Taylor expansion of the Brinkman friction expression with respect to polymer volume fraction, thus restricting the analysis to the case of polymer systems with sufficiently high water content (a situation recurrently met in practice). In eqn (1), we introduced $X = x/H$, $V(X) = v(x)/v_o$ with $v_o = \Delta P H^2/(\eta L_o)$ and η the dynamic viscosity of water. The function $\phi_o f(X)$ in eqn (1) corresponds to the adopted segment distribution $\phi(X)$ across the interface (Fig. 1), while $1/\lambda_o$ is the typical length scale pertaining to the extent of penetration of the tangential liquid flow within the PEO brush. The factor preceding $V(X)$ in eqn (1) describes how the friction exerted by the brush on the flow at the position X is connected to the corresponding segment density $\phi(X)$. In this work, we directly used the profiles $\phi_o f(X)$ obtained from the SCF theory for the evaluation of the hydrodynamic resistance of the brush. The streaming current I_{str}, caused by the pressure-driven flow of mobile charges at the PS/PEO/solution interphase, depends on the hydrodynamic flow field, $V(X)$ (eqn (1)), and the distribution of mobile ions in the interfacial region. Applying Boltzmann statistics for the ions distribution, I_{str} is given by:[27]

$$I_{str}/\Delta P = \frac{2\ell F H^3}{\eta L_o}\int_0^{1/2} V(X)\sum_{i=1}^{N} z_i c_i \exp(-z_i y(X))\,dX, \quad (2)$$

where N is the number of ion types of valence z_i, $y(X) = F\psi(X)/RT$ is the local dimensionless electrostatic potential evaluated from non-linear Poisson–Boltzmann equation, with ψ the potential, F the Faraday and R the gas constant.

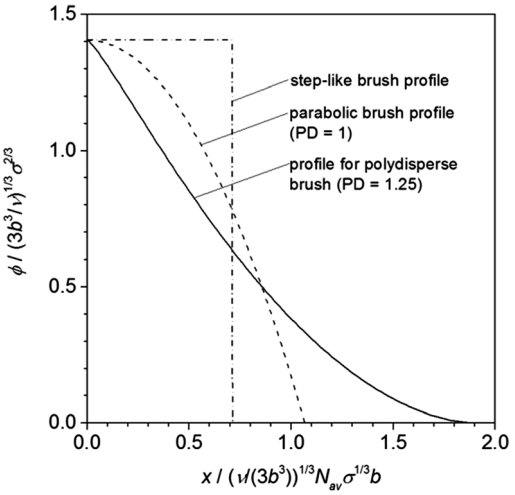

Fig. 1 Normalized density profile for a PEO brush with a polydispersity (PD) of 1.25. The parabolic profile, corresponding to a monodisperse brush (PD = 1), and the step-like profile with homogeneous density of polymer segments throughout the brush are shown for the sake of comparison. In line with the conditions of the electrokinetic experiments, the temperature was set to 295.15 K. For further details concerning profile calculation see text and ref. 28. The spatial coordinate x corresponds to the direction normal to the PEO/solution interphase.

4. Results and discussion

4.1 Brush profiles

To analyse the streaming current data presented in the next section, we first calculated the profiles for PD = 1 and PD = 1.25 (Fig. 1). For the sake of comparison, the profile of a brush with homogeneous density of polymer segments is shown in Fig. 1 as well.

For the monodisperse brush (PD = 1), we obtained the well-known parabolic profile.[6] In case of the polydisperse brush (PD = 1.25), the profile becomes convex and shows a distinct tail region where the brush density asymptotically approaches zero value.

The normalized brush profiles were converted into real segment distributions as described in Section 3.1. The excluded volume ν of the PEO monomer unit was the only unknown parameter that was adjusted for recovering the measured electrokinetic features of the PEO/electrolyte solution interphase *via* use of electrohydrodynamic theory for soft diffuse interfaces (next section). Typically ν is a function of the temperature and the volume fraction in the brush.[36–38] Because the latter dependence cannot be easily determined for the system of interest, we consider here that ν reflects the average excluded volume of the monomer units distributed throughout the PEO brush. Below we demonstrate how ν can be determined from the

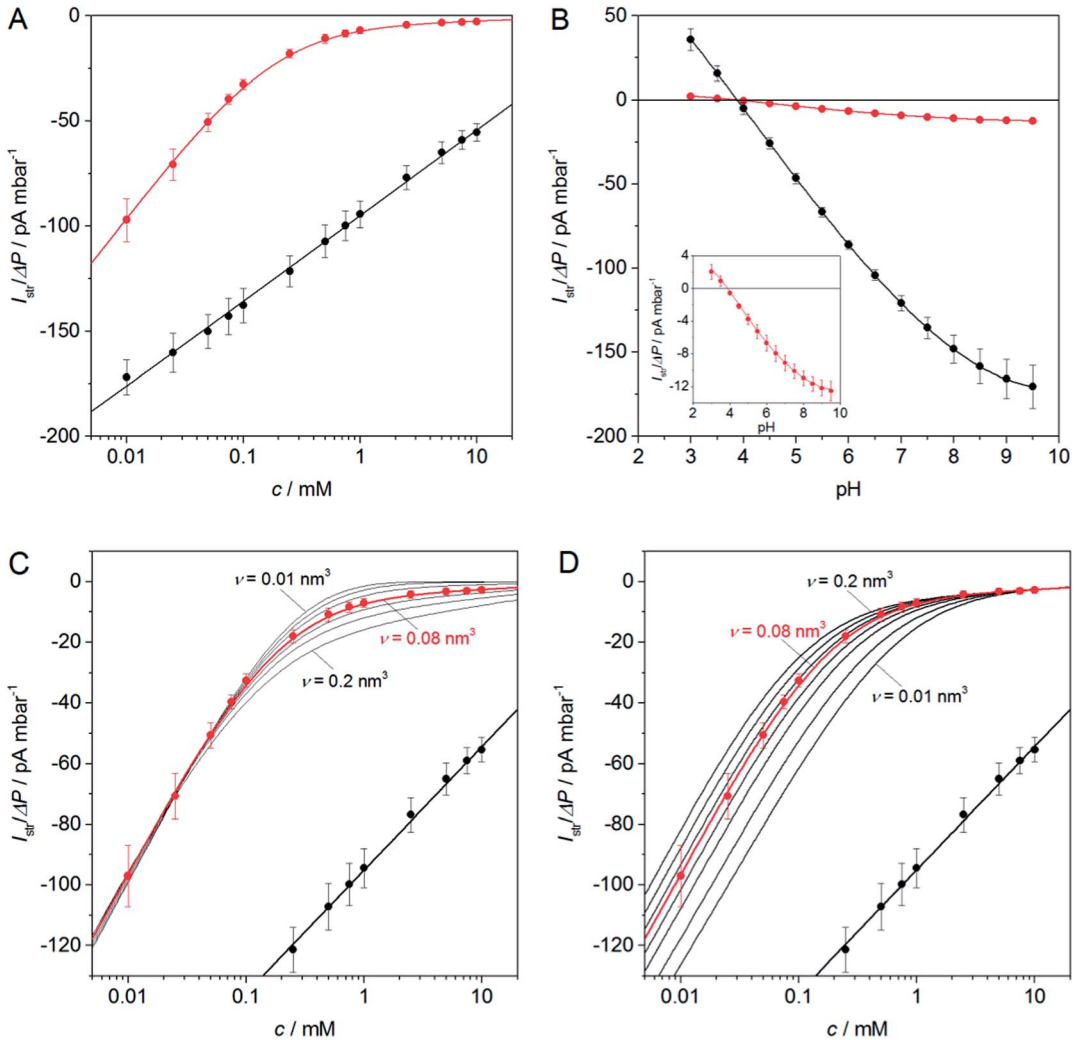

Fig. 2 Streaming current over applied pressure, $I_{str}/\Delta P$, as a function of KCl solution concentration at pH = 6 (A), as a function of pH in 1 mM KCl solution (B) for the bare PS-coated substrate (black) and in the presence of the PEO brush (red). Symbols with error bars pertain to experimental data, and solid lines to theoretical calculation obtained from eqn (1) and (2) adopting SCF profile at PD = 1.25 (Fig. 1). The strategy for the determination of the excluded volume parameter ν and the hydrodynamic penetration length $1/\lambda_o$ is illustrated in panels (C) and (D). The streaming current data were fitted in the range of low electrolyte concentrations (C), where the streaming current depends linearly on the logarithm of c, and in the range of high electrolyte concentrations (D), where the streaming current gradually tends to a zero value, for fixed values of the excluded volume parameter between 0.01 and 0.2 nm^3 (see ref. 36 and 41–43) by sole adjustment of the hydrodynamic penetration length $1/\lambda_o$. Adjustment was performed according to least mean square method and the searched couple (ν, $1/\lambda_o$) corresponds to that leading to the recovery of the experimental data over the entire range of KCl concentrations tested (red curves): $\nu = (0.08 \pm 0.01)$ nm^3 and $1/\lambda_o = (15.5 \pm 0.1)$ nm. Other model parameters: PD = 1.25, $b = 0.37$ nm, $\sigma = 0.1$ nm^{-2}, $N_{av} = 700$, $z = 1$, $T = 295.15$ K, $\varepsilon_r = 79.5$ (relative dielectric permittivity of the medium), $\eta = 0.954$ mPa s^{-1}, $H = 30$ μm, $\ell = 10$ mm, and $L_o = 20$ mm.

consistent reconstruction of streaming current data measured as a function of electrolyte concentration and pH.

4.2 Interfacial charging and structure

To analyse the interfacial charging and the impact of the PEO brush on the hydrodynamic ion transport along the PS/PEO/solution interphase, the streaming current was measured for the PEO brush and for the bare PS-coated substrate under 22 °C temperature condition at different KCl solution concentrations at pH = 6 (Fig. 2A) and at 1 mM KCl in the pH range 3 to 9.5 (Fig. 2B).[26] Regardless of the medium composition, the magnitude of $I_{str}/\Delta P$ for the bare carrier surface was significantly larger compared to that measured in the presence of the PEO brush. The isoelectric point (IEP) was found close to pH 4 for both the bare PS film and the PEO-coated PS substrate surface. Together with the whole pH-dependence of the streaming current, this IEP value typically reflects that the interfacial charge at the PS substrate surface stems from the unsymmetrical adsorption of hydroxide and hydronium ions.[39] In addition, minor differences between surface conductivities[26] and IEP values measured for the bare and PEO-coated PS surfaces strongly suggests that unsymmetrical adsorption of hydroxide and hydronium ions at the PS surface is not significantly affected by the presence of the PEO chains. The excess surface charge at the PS surface due to adsorbed water ions is screened by counter ions in the diffuse part of the electrical double layer. In case of the bare PS film, the compression of diffuse electrical double layer with increasing ionic strength[40] leads to a quasi-linear decrease of $|I_{str}/\Delta P|$ with increasing the logarithm of the KCl concentration. In the presence of grafted polymer chains, the magnitude of $|I_{str}/\Delta P|$ depends on the degree of screening of the PS surface charge by electrolyte ions (electrostatic screening) and by the propensity of the tangential flow to penetrate within the (uncharged) PEO brush (hydrodynamic screening).[21–24] As a result and in line with expectation from theory,[21–24] $|I_{str}/\Delta P|$ strongly decreases for KCl concentrations between 0.01 and 1 mM and asymptotically approaches zero value at higher electrolyte concentrations. This behaviour is the signature of the mixed electrostatic and hydrodynamic screening of the PS surface charge, resulting in a decrease of the amount of electrokinetically active ions in the vicinity of the charged PS surface.[21]

In order to reconstruct the experimental data shown in Fig. 2A by applying the theory outlined above, the streaming current data collected for the PS film in absence of the PEO brush were first converted into zeta potentials using the Helmholtz–Smoluchowski equation, thus providing the surface potential of the charged PS surface for evaluation of the potential distribution y involved in eqn (2).[40] Then, assuming that the interfacial charge formation is not impacted by the presence of the PEO brush (see ref. 18 and discussion above), the characteristic hydrodynamic penetration length $1/\lambda_o$ was solely adjusted for a given excluded volume ν in order to recover the experimental data in the low and high ionic strength regimes (Fig. 2C and D, respectively) where $I_{str}/\Delta P$ depends linearly on the logarithm of KCl concentration and gradually goes to zero, respectively. Examples are provided in Fig. 2C and D for selected values of ν, recalling that for a given ν the adopted segment density distribution is independently provided by SCF computation with PD = 1.25. It is emphasized that variations in ν affect the spatial extension of the brush and the local segment density distribution therein (Fig. 1). In turn, they modulate the friction force exerted by the brush on the tangential flow and thus the magnitude of the streaming current (eqn (1) and (2)). The reader is referred to ref. 21 and 22 for further details on the dependence of the streaming current on $1/\lambda_o$ and on the interphasial gradient in segment density (determined here by the nature of the profile adopted, in particular by the quantities PD and ν). The searched couple (ν, $1/\lambda_o$) is that leading to a recovery (according to least square method) of $I_{str}/\Delta P$ over the entire range of KCl concentrations tested. The best fit was obtained for $\nu = (0.08 \pm 0.01)$ nm^3 and $1/\lambda_o = (15.5 \pm 0.1)$ nm (red curves in Fig. 2C and D). Most of the values published for the excluded volume of the PEO monomer unit are slightly lower or very close to the volume of the PEO monomer unit (0.0646 nm^3),[36,41–43] which is in line with our result. Possible reasons for the observed minor difference could result from the inherent approximations of the mean-field Poisson–Boltzmann equation.[21–27] The consistency of the introduced methodology is further confirmed by the reproduction of the data in Fig. 2B. Indeed, with fixing the quantities ν and $1/\lambda_o$ determined according to the above procedure, the theoretical prediction for the dependence of $I_{str}/\Delta P$ on pH in 1 mM KCl very well agrees with the electrokinetic data measured under such conditions (Fig. 2B). It is emphasized that the comparison experiment-theory in Fig. 2B does not require any further adjustment of model parameters. As the brush profile was independently evaluated according to SCF theory at given ν, the results of Fig. 2 illustrate the high sensitivity of the streaming current for probing structural details of diffuse soft interphases.

The strategy above was followed to attempt a recovery of the electrokinetic data using the parabolic and step-like profiles depicted in Fig. 1 for $\phi(X)$. For both profiles, the merging between experiments and theory could be achieved only with physically unrealistic values of ν ($\nu \sim (0.22 \pm 0.02)$ nm^3 and $\nu \sim (0.35 \pm 0.02)$ nm^3 for the parabolic and step-function distributions, respectively). To illustrate the impact of the brush profile on the streaming current, simulated curves at $\nu = 0.08$ nm^{-3} (as determined using the SCF brush profile corresponding to PD = 1.25) are further reported in Fig. 3 with $1/\lambda_o$ values that best reproduce electrokinetic data at low and high ionic strengths for hypothetical parabolic and step-like density profiles (Fig. 3A and B, respectively). The corresponding results further strengthen the suitability of electrokinetics to capture differences in brush density profiles.

The extension h of the polydisperse brush can be evaluated from the relationship used for the normalization of the x-axis in Fig. 1. With $\nu = 0.08$ nm^3, $b = 0.37$ nm, $\sigma = 0.1$ nm^{-2} and $N_{av} = 700$, we obtain $h \approx 94$ nm. The ratio between h and the hydrodynamic penetration length $1/\lambda_o$ is therefore $h\lambda_o \approx 6.1$. In addition, the electrolyte concentrations tested in this work correspond to electric double layer thickness $1/\kappa$ in the range 96 nm (in 0.01 mM KCl) to 3 nm (in 10 mM KCl) so that the ratio

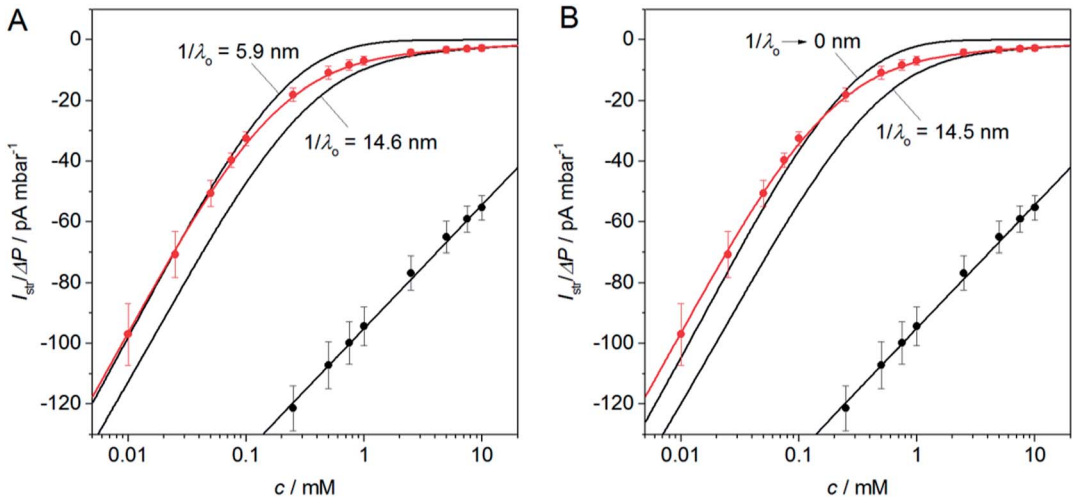

Fig. 3 Streaming current over applied pressure, $I_{str}/\Delta P$, as a function of KCl concentration, c, for PEO brushes with hypothetical parabolic (left) and step-like (right) density profiles (symbols: experimental data, black solid lines: theoretical calculation obtained from eqn (1) and (2)). The parabolic profile (PD = 1) was evaluated with $\nu = 0.08$ nm^3. The best fit line obtained with adopting the SCF density profile for PD = 1.25 is shown in red for the sake of comparison. Using the parabolic or step-like density profile, it is impossible to completely recover the electrokinetic data upon adjustment of $1/\lambda_o$, as indicated. Other model parameters: as in Fig. 2.

between $1/\kappa$ and $1/\lambda_o$ varies between 6.2 and 0.2 under the salinity conditions adopted in our work. These estimations illustrate that the number of electrokinetically active counter ions located within the brush significantly decreases with increasing salinity. In addition, the electrokinetic analysis done in this study for the specific case of brush systems reveals details of polymer profile distribution provided that the polymer layer thickness is comparable to the Debye screening length (or of the same order of magnitude, for further details see ref. 21–24). This situation is met here over a large range of ionic strength conditions.

4.3 Are subtle differences in the PEO brush profile resolved in neutron reflectivity curves?

In order to firmly address the applicability of neutron reflectivity measurements to probe efficiently any differences in the brush structure as correctly detected by electrokinetics, neutron reflectivity profiles were computed for PEO brushes with step-like profile and SCF profiles for PD = 1 and PD = 1.25 adopting $\nu = 0.08$ nm^{-3} and applying the theory by Fermon (Fig. 4).[44] Computations were performed with use of the DLreflec function from the PASINET library developed by D. Lairez from LLB, Grenoble.[45] Briefly, scattering profiles were evaluated for a multilayer system consisting of a silicon substrate, a 1 nm thick SiO_2 layer, a 2 nm thick PS film, the PEO brush and an adjacent D_2O phase (which offers a better contrast than H_2O in terms of their respective neutron scattering length density compared to that of PEO). The scattering length densities corresponding to the different materials of interest were (in 10^{10} cm^{-2}): b_B (Si) = 2.07, b_B (SiO_2) = 3.47, b_B (PS) = 1.42, b_B (PEO) = 0.64, and b_B (D_2O) = 6.36 and the position dependence of the scattering length density across the brush was formulated according to b_B (PEO) × $\phi(X)$ + b_B (D_2O) × (1 − $\phi(X)$).

In case of a hypothetical step-like brush profile, a clear interference pattern (Kiessing fringes) was obtained (Fig. 4), which makes it possible to determine the brush height and the polymer surface concentration.[44,46] This determination is however practically impossible upon introducing interfacial roughness in the modelling,[14] because it leads to a destruction of the fringes.

In addition, reflectivity curves for the parabolic and SCF-brush profiles are quasi-identical and do not exhibit interference fringes (Fig. 4), which, in turn, does not allow for an unambiguous evaluation of the brush profile. This result strongly supports the so-far overlooked benefits offered by the

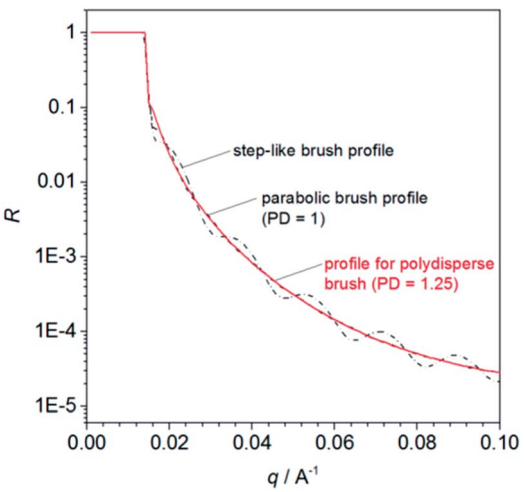

Fig. 4 Neutron reflectivity, R, *versus* scattering vector, q, computed for step-like brush profile and SCF brush profiles for PD = 1 (parabolic profile for monodisperse brush) and PD = 1.25 (polydisperse brush) with $\nu = 0.08$ nm^{-3}.

consistent analysis of brush electrokinetic features with applying electrohydrodynamic theory for diffuse soft interphases.

5. Conclusion

The analysis of streaming current measurements with combined SCF and soft surface electrokinetic theories provides detailed information on the segment distribution within polydisperse polymer brushes. Because of the low segment density in the tail region, these differences cannot be resolved by neutron reflectivity technique. The introduced methodology can be applied for uncharged brushes under conditions where the brush thickness is comparable to the Debye screening length at low ionic strength conditions. The structural details derived by this approach could be helpful for better understanding functional properties and interactions of brushes in cutting edge technologies, *e.g.* in micro and nanofluidics and biomedical engineering. Future work will be dedicated to the incorporation of molecular details in soft surface electrokinetic theory for brushes with ionisable groups whose chemical environment will be explicitly accounted for, together with the local fluctuation of the polymer chains.

References

1 S. T. Milner, *Science*, 1991, **251**, 905.
2 E. P. K. Currie, W. Norde and M. A. Cohen Stuart, *Adv. Colloid Interface Sci.*, 2003, **102**, 206.
3 S. Minko, *J. Macromol. Sci., Part C: Polym. Rev.*, 2006, **46**, 397.
4 S. Alexander, *J. Phys.*, 1977, **38**, 983.
5 P.-G. de Gennes, *Macromolecules*, 1988, **13**, 1069.
6 S. T. Milner, T. A. Witten and M. E. Cates, *Macromolecules*, 1988, **21**, 2610.
7 C. M. Wijmans, J. M. H. M. Scheutjens and E. B. Zhulina, *Macromolecules*, 1992, **25**, 2657.
8 C.-M. Chen and Y.-A. Fwu, *Phys. Rev. E: Stat., Nonlinear, Soft Matter Phys.*, 2000, **63**, 011506.
9 D. Bedrov and G. D. Smith, *Langmuir*, 2006, **22**, 6189.
10 H. Ahrens, S. Förster and C. A. Helm, *Phys. Rev. Lett.*, 1998, **81**, 4172.
11 P. Auroy, Y. Mir and L. Auvray, *Phys. Rev. Lett.*, 1992, **69**, 93.
12 R. Toomey, D. Freidank and J. Rühe, *Macromolecules*, 2004, **37**, 882.
13 M. J. N. Junk, I. Anac, B. Menges and U. Jonas, *Langmuir*, 2010, **26**, 12253.
14 E. P. K. Currie, M. Wagemaker, M. A. Cohen Stuart and A. A. van Well, *Macromolecules*, 1999, **32**, 9041.
15 S. S. Dukhin, N. M. Semenikkin and W. A. Bychko, in *Surface forces in thin layers*, ed. B.V. Derjaguin, Acad. Science USSR, Nauka, Moskow, 1979, pp. 85–93, (in Russian).
16 M. A. Cohen Stuart, F. H. W. H. Waajen and S. S. Dukhin, *Colloid Polym. Sci.*, 1984, **262**, 423.
17 H. Ohshima and T. Kondo, *J. Colloid Interface Sci.*, 1990, **135**, 443.
18 V. M. Starov and Y. E. Solomentsev, *J. Colloid Interface Sci.*, 1993, **158**, 159.
19 J. F. L. Duval and H. P. van Leeuwen, *Langmuir*, 2004, **20**, 10324.
20 L. Yezek, J. F. L. Duval and H. P. van Leeuwen, *Langmuir*, 2005, **21**, 6220.
21 J. F. L. Duval, R. Zimmermann, A. L. Cordeiro, N. Rein and C. Werner, *Langmuir*, 2009, **25**, 10691.
22 R. Zimmermann, D. Kuckling, M. Kaufmann, C. Werner and J. F. L. Duval, *Langmuir*, 2010, **26**, 18169.
23 J. F. L. Duval, D. Küttner, M. Nitschke, C. Werner and R. Zimmermann, *J. Colloid Interface Sci.*, 2011, **362**, 439.
24 J. F. L. Duval, D. Küttner, C. Werner and R. Zimmermann, *Langmuir*, 2011, **27**, 10739.
25 R. Zimmermann, S. Bartsch, U. Freudenberg and C. Werner, *Anal. Chem.*, 2012, **84**, 9592.
26 R. Zimmermann, W. Norde, M. A. Cohen Stuart and C. Werner, *Langmuir*, 2005, **21**, 5108.
27 R. Zimmermann, S. S. Dukhin, C. Werner and J. F. L. Duval, *Curr. Opin. Colloid Interface Sci.*, 2013, **18**, 83.
28 S. T. Milner, T. A. Witten and M. E. Cates, *Macromolecules*, 1989, **22**, 853.
29 E. P. K. Currie, J. van der Gucht, O. V. Borisov and M. A. Cohen Stuart, *Pure Appl. Chem.*, 1999, **71**, 1227.
30 C. Werner, H. Körber, R. Zimmermann, S. S. Dukhin and H.-J. Jacobasch, *J. Colloid Interface Sci.*, 1998, **208**, 329.
31 R. Zimmermann, T. Osaki, R. Schweiss and C. Werner, *Microfluid. Nanofluid.*, 2006, **2**, 367.
32 W. M. de Vos, PhD Thesis, Wageningen University, 2009.
33 E. P. K. Currie, F. A. M. Leermakers, M. A. Cohen Stuart and G. J. Fleer, *Macromolecules*, 1999, **32**, 487.
34 W. M. de Vos and F. A. M. Leermakers, *Polymer*, 2009, **50**, 305.
35 H. C. Brinkman, *Appl. Sci. Res.*, 1947, **A1**, 27.
36 R. Xu, M. A. Winnik, G. Riess, B. Chu and M. D. Croucher, *Macromolecules*, 1992, **25**, 644.
37 V. A. Baulin, E. B. Zhulina and A. Halperin, *J. Chem. Phys.*, 2003, **119**, 10977.
38 V. A. Baulin and A. Halperin, *Macromol. Theory Simul.*, 2003, **12**, 549.
39 R. Zimmermann, U. Freudenberg, R. Schweiß, D. Küttner and C. Werner, *Curr. Opin. Colloid Interface Sci.*, 2010, **15**, 196.
40 J. Lyklema, *Fundamentals of Colloids and Interface Science: Solid-Liquid Interfaces*, vol. 2, Academic Press, London, 1991.
41 K. Devanand and J. C. Selser, *Macromolecules*, 1991, **24**, 5943.
42 E. E. Dormidontova, *Macromolecules*, 2002, **35**, 987.
43 B. Lonetti, A. Tsigkri, P. R. Lang, J. Stellbrink, L. Willner, J. Kohlbrecher and M. P. Lettinga, *Macromolecules*, 2011, **44**, 3583.
44 C. Fermon, *J. Phys. IV*, 2001, **11**, Pr9–33.
45 http://didier.lairez.fr/dokuwiki/doku.php?id=traitement_et_analyse:modelisation_des_donnees:reflectivite.
46 G. Fragneto-Cusani, *J. Phys.: Condens. Matter*, 2001, **13**, 4973.